


RESEARCH ARTICLE

Utilization of iron scrap into copperas and rambutan (*Nephelium lappaceum* L.) peel extract into environmentally friendly iron nanoparticles for hexavalent chromium removal and its kinetics

Sunardi Sunardi¹  | Sumardiyono Sumardiyono² | Mardiyono Mardiyono³ | Nur Hidayati⁴ | Soebiyanto Soebiyanto⁴

¹Chemical Analyst Study Program, Faculty of Engineering, Setia Budi University, Surakarta, Indonesia

²Chemical Engineering Study Program, Faculty of Engineering, Setia Budi University, Surakarta, Indonesia

³Pharmacy Study Program, Faculty of Pharmacy, Setia Budi University, Surakarta, Indonesia

⁴Health Analyst Study Program, Faculty of Health Science, Setia Budi University, Surakarta, Indonesia

Correspondence

Sunardi Sunardi, Chemical Analyst Study Program, Faculty of Engineering, Setia Budi University, Surakarta, Indonesia.

Email: sunardi@setiabudi.ac.id

Abstract

Hexavalent chromium is a toxic pollutant that is very harmful to human health and the environment. One of the materials for hexavalent chromium removal is iron nanoparticles (INPs). In recent years, the manufacture of environmentally friendly INPs has been of great interest. In general, INPs are made using sodium tetra borane/ NaBH_4 , which is expensive. The synthesis of INPs using NaBH_4 also produces side products in the form of toxic boric acid and hydrogen gas which are explosive and flammable. In this study, INPs are made by using iron scrap waste into copperas which is then reacted with rambutan peel extract (RPE). The reaction between iron scrap and sulfuric acid until crystals are formed and then washed until blue-green crystals are formed. The resulting crystal is made into a solution and then reacted with RPE. After forming a black solution, it was dried by spray drying. The resulting black powder was characterized by UV-Vis Spectrophotometer, SEM-EDX, FTIR, and XRD. The results showed that iron scrap can be synthesized into copperas with a Fe content of $19.84 \pm 0.15\%$. RPE has a total phenol content of 877.39 ± 16.6 ppm/100 g rambutan skin or equivalent to 441.42 mg GAE/100 g rambutan skin. INPs can be made from copperas from iron scrap and RPE which have Surface Plasmon Resonance (SPR) characteristics at 214 nm absorption, particle size 20–70 nm. Hexavalent chromium removal using INPs was maximum at pH 3, hexavalent chromium concentration of 5 ppm, INPs concentration of 0.15 g/100 mL, and contact time of 10 min. The adsorption isotherm type of hexavalent chromium using iron nanoparticles can take place chemically or physically. The correlation coefficient showed that the model of Freundlich ($R^2 > 0.99$) is more suitable than the model of Langmuir ($R^2 = 0.98$) with an adsorption capacity of 91.74 mg iron nanoparticles/g hexavalent chromium. The use of INPs for hexavalent chromium removal is a promising and effective technology. These results can be an alternative to the production of environmentally friendly INPs by using materials from waste into useful materials for the prevention of environmental pollution.

KEYWORDS

environmentally friendly, iron nanoparticles, iron scrap, rambutan peel extract

1 | INTRODUCTION

In recent years, research on iron nanoparticles (INPs) has received great attention. This is because nanoparticles are an important material to overcome environmental pollution. The use of INPs is very broad including for the treatment of water, wastewater, wells, soil, sediment, and gas flow (Machado et al., 2013). The. For instance, ciprofloxacin, sulfamethoxazole technology of using INPs provides potential advantages over conventional methods due to their unique physicochemical properties, non-toxicity, and economics (Etemadi et al., 2017; Fazlzadeh et al., 2017; Poguberović et al., 2016; Ravikumar et al., 2016). The main advantage of this technique is that relatively simple using only two reagents and no need for specialized equipment. In addition, since it is very small, it can be effectively injected and transported into groundwater and polluted aquifers in situ treatment (Chang et al., 2014; Chen et al., 2015; Li et al., 2017; Madhavi et al., 2013). The pollutant that can be remediated by INPs include azo compounds, chlorinated pesticides, chlorinated solvents, transition metals, and inorganic anions (Crane & Scott, 2012), inorganic and organic pollutants (Shahwan et al., 2011), heavy metals (Li et al., 2017; Yuan et al., 2016), nitrate (Wang et al., 2014), bromide (Xu et al., 2015), arsenic (Poguberović et al., 2016; Prasad et al., 2014), hexavalent chromium (Chen et al., 2015; Jiao et al., 2015; Poguberović et al., 2016; Ravikumar et al., 2016; Sheng et al., 2016), lead (Kumari et al., 2015), antibiotics (Leili et al., 2018), and colorants (Fujioka et al., 2016). INPs are also used in cosmetics, biomedicine, bioremediation, clinical materials, and engineering (Harshiny et al., 2015). INPs have unique properties such as small particle size, and large surface area, making them highly reactive (Mystrioti et al., 2016; O'Carroll et al., 2013), catalytic and optical, electronic and antibacterial activities (Harshiny et al., 2015; Kokila et al., 2015; Saif et al., 2016).

The technology of using INPs provides potential advantages over conventional methods due to their unique physicochemical properties, non-toxicity, and economics

Nanoparticle production is generally categorized into two groups: top-down and bottom-up approaches. The top-down approach is to break down large particles into nanometer-size particles. The bottom-up approach is to start with atoms or molecules or clusters that are engineered to form the desired nanometer-size particles (Devatha et al., 2016; Saif et al., 2016). Synthesis of INPs with a top-down approach including the preparation of nanoparticles by physical methods, thermal breakdown, sonochemical synthesis, and vacuum sputtering. These methods have limitations, namely, low production rates,

high temperatures and pressures, or high energy requirements, making them relatively expensive (Devatha et al., 2016; Mo et al., 2015; Wang et al., 2017).

Production of INPs with an approach of a bottom-up including production methods of traditional. Some methods of traditional methods of producing INPs include coprecipitation (Petcharoen & Sirivat, 2012; Yoon et al., 2014), hydrothermal method (Giri et al., 2005), and hydrolysis (Tsang et al., 2006). In general, the preparation of INPs is done by reducing iron valence $\text{Fe}^{3+}/\text{Fe}^{2+}$ with sodium tetra borane (NaBH_4) (Prasad et al., 2014). Preparation of INPs using NaBH_4 produces toxic boric acid and hydrogen gas as by-products that are easily explosive and flammable (Ahamed et al., 2016; Devatha et al., 2016; Saif et al., 2016).

Meanwhile, lathe activities produce waste in the form of iron chips. Solid waste from the lathe workshop has been mostly utilized for recycled iron with mark very low economy value. Iron powder from the lathe workshop which is very small in size is usually not utilized anymore, disposed of directly and this causes environmental pollution. The waste still contains valuable materials that when recycled can provide an economic return, namely, with the principles of reuse, recycling, and recovery.

On the other hand, rambutan fruit skin is waste that is simply thrown away. Rambutan peels contain bioactive compounds such as polyphenols (Anouar et al., 2015; Isacfranklin et al., 2020; Karnan et al., 2016; Karnan & Selvakumar, 2016; Mendez-Flores et al., 2018; Thitilertdecha & Rakariyatham, 2011; Thitilertdecha et al., 2010; Yuvakkumar et al., 2015; Zhuang et al., 2017). Polyphenols are compounds that can reduce Fe^{2+} to Fe^0 (Leili et al., 2018; Solimanzadeh et al., 2016; Wei et al., 2016). The amount of rambutan peel is about 25% of whole fruit and is a waste product is a potential material as a source of polyphenols (Karnan & Selvakumar, 2016; Kumar et al., 2016; Thitilertdecha et al., 2008, 2010), which can be used for the manufacture of environmentally friendly INPs. The polyphenol content in RPE is thought to be able to reduce Fe^{2+} from copperas to INPs.

The general objective of this research is to remove hexavalent chromium using INPs synthesized from RPE and ferrous sulfate from iron waste. The general objective can be achieved by answering the specific objectives, namely: (1) determining the copperas content of iron scrap, (2) determining the total phenol content of RPE, (3) characterizing INPs made from copperas base of iron scrap and RPE, and (4) reducing hexavalent chromium using INPs synthesized from RPE and ferrous sulfate from iron waste.

2 | MATERIALS AND METHODS

The materials used in the study were iron scrap taken from a lathe workshop. The rambutans were bought from the fruit market. Iron nanoparticle samples were obtained by reacting copperas from iron scrap with rambutan peel extract (RPE). The source of chromium was Potassium Chromate (K_2CrO_4) from Sigma Aldrich. The source of concentrated sulfuric acid for making copperas from Merck. The tools used in research are UV-Vis Spectrophotometer (Shimadzu

UV-1650pc Spectrophotometer), Scanning Electron Microscope-Electron Dispersive X-Ray Spectroscopy (SEM-EDX) brand Shimadzu type 600, Fourier Transform Infra Red (FTIR, Nicolet 6700, USA), and X-Ray Diffraction (XRD) Shimadzu type 600.

The materials used in the study were iron scrap taken from a lathe workshop

2.1 | Preparation and determination of copperas content from iron scrap

Preparation of copperas from iron scrap from the lathe workshop as follows: Approximately 25 g of clean iron scrap was reacted with 100 mL of 25% sulfuric acid in an Erlenmeyer. The solution was filtered and then put in the refrigerator for 24 h. The crystals formed were filtered with a vacuum pump and then washed with alcohol. The crystals formed were dried in a desiccator. Determination of levels was carried out by UV-Vis Spectrophotometer.

2.2 | Preparation of rambutan peel extract (RPE) and determination of phenol total content

Preparation of RPE as a source of polyphenols using the method by Kokila et al. (2015). The 100 g rambutan peel was cut into small pieces with a size of ± 0.5 cm and boiled in distilled water for 90 min at a temperature of $\pm 800^\circ\text{C}$. The ratio of rambutan peel mass to water mass is 1:3. The filtrate was filtered with a filter cloth, then with Whatman paper no. 1 on vacuum filtration. A qualitative test for phenol was done by looking at the presence of the OH group using FTIR at $3200\text{--}3550\text{ cm}^{-1}$ (Kokila et al., 2015).

2.3 | Preparation and characterization of INPs

Preparation of INPs was carried out using copperas from iron scrap and RPE. For the preparation of INPs, the copperas solution used was 5 mL of 0.001 M added to 5 mL of RPE. The reaction was carried out with constant stirring and at room temperature for 5 min (Anouar et al., 2015). The formation of a black solution indicates the formation of INPs (Fazlzadeh et al., 2017; Harshiny et al., 2015; Karnan & Selvakumar, 2016; Kumar et al., 2015; Machado et al., 2013; Noruzi & Mousivand, 2015; Ravikumar et al., 2016; Shahwan et al., 2011; Wei et al., 2016). The formed colloidal INPs were dried by spray drying. The crystals formed were characterized by UV-Vis Spectrophotometer, SEM-EDX, FTIR, and XRD.

2.4 | Determination of efficiency and adsorption type of hexavalent chromium removal by INPs

In each experiment, 100 mL of hexavalent chromium solution (5, 10, 15) ppm was added (0.01, 0.05, 0.1, 0.15) g INPs, varying pH (3, 7, 11). The mixture was stirred with a stirring speed of 150 rpm at room temperature and time variations (3, 5, 10, 15, 20, and 30) min. The concentration of hexavalent chromium in the filtrate was analyzed using 1,5 diphenyl-carbazide and measured by UV-Vis spectrophotometer at a wavelength of 540 nm. The adsorbed hexavalent chromium was calculated from the initial hexavalent chromium concentration minus the hexavalent chromium concentration after adsorption in the filtrate. The performance of INPs was determined by constructing a curve between the percentage of hexavalent chromium adsorbed and contact time.

The hexavalent chromium removal percentage was calculated by the formula:

$$\% \text{ Removal} = \frac{C_i - C_f}{C_i} \times 100\% \quad (1)$$

The optimum results of the performance test of iron nanoparticles that have been obtained are then removed with variations in adsorbate concentration to determine the type of adsorption isotherm. Into five 250 mL beakers, each filled with 0.1 g of iron nanoparticles at optimum conditions, then added hexavalent chromium solution with a concentration of (5, 10, 15, 20, 25) ppm 100 mL as the initial concentration (C_0), then stirred at the optimum time. The removal results were filtered, and then the filtrate was measured for hexavalent chromium content with a UV-Vis spectrophotometer (C_e).

The adsorption capacity (q_e , mg/g) was calculated by Equation (2):

$$q_e = \frac{C_0 - C_e}{m} \times V \quad (2)$$

$V(L)$, volume of solution chromium hexavalent, m (mg) for mass INPs.

The Freundlich and Langmuir isotherms are used to explain the balance between adsorbate and adsorbent using Equations (3) and (4).

$$\log q_e = \log K_f + \frac{1}{n} \log C_e \quad (3)$$

$$\frac{C_e}{q_e} = \frac{1}{q_{max} \cdot b} + \frac{C_e}{q_{max}} \quad (4)$$

caption,

q_e , mass adsorbate adsorbed by the adsorbent (mg/g)

K_f , factor Freundlich capacity (determined by q_e)

C_e , the equilibrium concentration adsorbate in phase liquid after adsorption (mg/L)

n , the Freundlich intensity parameter

q_{max} , the amount of maximum possible adsorbate absorbed (mg/kg)

b is constant Langmuir isotherm.



EXHIBIT 1 Iron scrap and copperas from iron scrap. [Color figure can be viewed at wileyonlinelibrary.com]

EXHIBIT 2 Determination of copperas content of scrap iron.

Rate determination	λ_{\max} (n.m.)	absorbance	[Fe ²⁺] (ppm)	Weight Fe ²⁺ (mg)	Fe ²⁺ content (%)	Copperas weight (mg)	Copperas content (%)
1	510	0.096	0.47	59,10	19.73	294,21	98.23
2		0.097	0.48	59,77	19.94	297.53	99.27
Average (x)					19.84		98.75
Standard deviation (s)					0.15		0.74

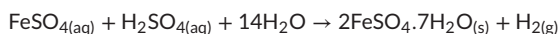
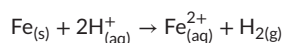
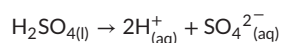
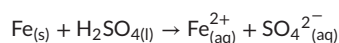
Then made a graph $\log q_e$ to the $\log C_e$ for the Freundlich and C_e/q_e isotherms to C_e for Langmuir isotherm.

3 | RESULTS AND DISCUSSION

3.1 | Preparation and determination of copperas content

The reaction between iron scrap from the lathe workshop and 25% sulfuric acid produced blue-green crystals as shown in Exhibit 1.

The reaction for making copperas from iron scrap and sulfuric acid is:



The determination results from copperas levels from iron scrap was done with the use of spectrophotometry Uv -Vis as shown in Exhibit 2.

Exhibit 2 shows that the average Fe²⁺ content in copperas is $19.84 \pm 0.15\%$ while the average content of copperas from iron scrap

is $98.75 \pm 0.74\%$. This shows that the copperas synthesized from iron scrap in the lathe workshop meet the quality requirements of copperas SNI 06-4888-1998 which requires a minimum Fe content of 19% (BSN, 1998; Valentovic, 2007).

3.2 | Determination of total phenolics of rambutan peel extract

Exhibit 3 shows the results of the calculation of total polyphenol content of RPE.

Exhibit 3 shows that the average TPC was 877.40 ± 16.6 ppm/100 g rambutan peel. So the total polyphenol content in RPE is 877.39 ± 16.6 ppm.

The total phenol concentration in the extract was then used for the calculation of the equivalent organic carbon concentration in the extract, OC (GAE), in mg C/L, by considering the presence of a carbon atom in each gallic acid molecule, according to the following equation:

$$\text{OC (GAE)} = \left[\frac{\text{TPC}}{M} \right] \times 7 \times 12 \text{ g/mol}$$

description:

TPC: Total Phenolic Content (total polyphenol concentration) (mg GAE/L)

M: molecular weight of gallic acid (C₇H₆O₅), equal to 170.12 g/mol

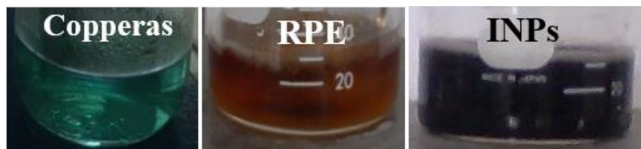
7: Number of carbon atoms in each gallic acid molecule

12 g/mol: Weight of carbon atoms

(Mystrioti et al., 2016). Based on the calculation results, the total phenol content in RPE is 441.43 mg GAE/100 g rambutan skin.

EXHIBIT 3 Total phenol content of RPE.

Rate determination	Δ_{\max} (n.m.)	Absorbance	Total phenol concentration (ppm)	Phenol content (ppm)
1	765	0.435	35.5652	889.1304
2		0.425	34.6261	865.6521
Average (x)				877,3913
Standard deviation (s)				16,6

**EXHIBIT 4** Reaction between copperas solution and RPE to produce INPs. [Color figure can be viewed at wileyonlinelibrary.com]

3.3 | Preparation and characterization of INPs

The reaction between copperas solution and RPE synthesized produces a black solution as shown in Exhibit 4.

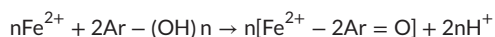
When RPE was reacted with a solution of copperas, the color of the solution changed rapidly to black from brown, and a precipitate formed as shown in Exhibit 4. The same event also occurred in the reaction of orange peel extract with FeCl_3 (Wei et al., 2016), green tea extract, cloves, mint plants, pomegranate, and red wine with FeCl_3 and neem leaves with $\text{FeSO}_4 \cdot 7\text{H}_2\text{O}$ (Ravikumar et al., 2016). This shows that there has been a reaction between Fe^{2+} ions from copperas with polyphenols from RPE to form INPs.

The formation of INPs from RPE can also be proven by observing the formation of SPR (Surface Plasmon Resonance). SPR is a resonance phenomenon between visible light waves and electrons on a metal surface that produces oscillations of electrons on the quantized metal surface. Exhibit 5 shows the absorption analysis spectra of the SPR peak at 214 nm absorption.

These results are similar to published studies at 214 nm (Harshiny et al., 2015), 216 nm absorption, and 211 nm (Ravikumar et al., 2016).

Polyphenols form INPs with the following steps: (a) formation of Fe complex compounds, (b) simultaneous Fe^{2+} ion reduction, and (c) oxidized capping. Thus, the mechanism of iron nanoparticle formation from rambutan peel extract is as follows:

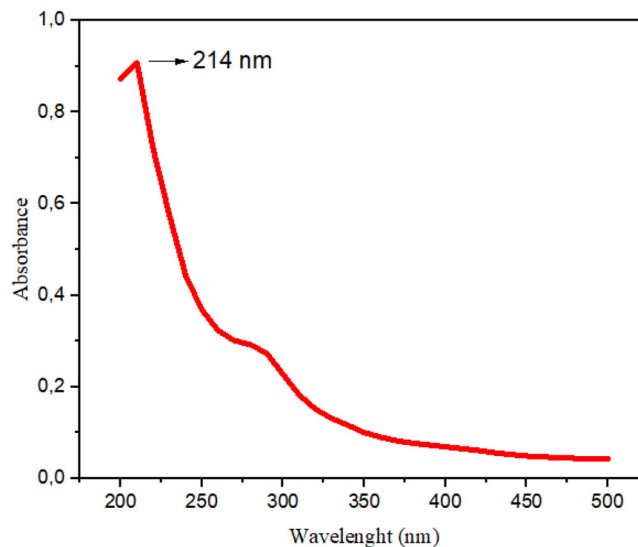
(1) Formation of complex compounds



(2) Simultaneous reduction of Fe^{2+}

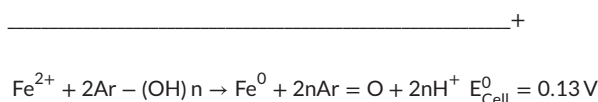
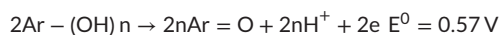
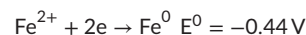


(3) Prevention of oxidation

**EXHIBIT 5** UV-Vis SPR spectra of INPs resulting from the reaction of copperas with RPE. [Color figure can be viewed at wileyonlinelibrary.com]

$2(x + 1)\text{Fe}^0 + 2\text{Ar} = \text{O} + y\text{O}_2 \rightarrow 2(\text{Fe}^0 - \text{FexOy} - \text{Ar} = \text{O})$ (Wang et al., 2014).

In stages (1) and (2) of INP formation, polyphenols form complexes directly and then reduce Fe^{2+} ions (valence 2) to Fe^0 (valence 0). The process of reduction and oxidation reactions depends on the reduction potential (E^0) of each reagent. According to Wang et al. (2017), polyphenols have a reduction potential of 0.57 V sufficient to reduce Fe^{2+} to Fe^0 which has a reduction potential of -0.44 V.



A reaction can be said to be spontaneous if it meets the thermodynamic requirements, namely, its Gibbs free energy (ΔG°) < 0 . The value of ΔG° can be determined from the standard cell potential by the

EXHIBIT 6 Elemental content test results of INPs.

Elements	keV	Mass %	Sigma
CK	0.277	25,32	0.12
NK	0.392	7,68	0.17
OK	0.525	45,36	0.26
PK	2.013	0.63	0.02
SK	2307	1.20	0.02
KK	3312	0.17	0.01
Fe K	6398	19,64	0.13
Total		100.00	

formula:

$$\Delta G^{\circ} = -nFE_{\text{Cell}}^{\circ}$$

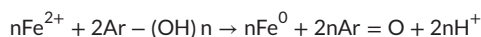
Description:

ΔG° , Gibbs free energy

n , number of electrons involved,

F , Faraday's constant, $96500 \text{ C}\cdot\text{mol}^{-1}$

If a cell has a positive E_{Cell}° price, then the ΔG° price will be negative and the reaction will be spontaneous. Therefore, the reaction between RPE and Fe^{2+} ions is spontaneous. This can be seen when the copperas and RPE solutions are mixed, there is an immediate reaction to form INPs (black solution) as shown in Exhibit 4. In general, the reaction mechanism for the synthesis of INPs with polyphenols is:



Ar is a group of phenyl and n is the number of OH groups that reduce Fe^{2+} (Mystrioti et al., 2016; Wang et al., 2017).

At stage (3), in the form of an RPE solution, capping and stabilization by polyphenols occur so that Fe° is not oxidized. The presence of capping containing Fe, C, and O elements is also shown by SEM-EDX analysis results (Exhibits 6 and 7).

Exhibit 6 shows intense peaks indicating the presence of Fe, C, and O. The elements involved in the formation of INPs are shown in Exhibit 7, namely, O (45.36%), C (25.32%), Fe (19.64%), N (7.68%), S (1.20%), P (0.63%), and K (0.17%). The presence of Fe, C, and O is a sign that INPs have been successfully synthesized from RPE. This result is similar to the published research by Wang et al. (2017), Noruzi and Mousivand (2015), and Ravikumar et al. (2016).

SEM analysis results in the form of INPs as shown in Exhibit 8.

In Exhibit 8, it can be seen that most of the iron nanoparticles are round with a size of 10–70 nm. These results are similar to those of Machado et al. (2013), Poguberović et al. (2016), and Wei et al. (2016). Smaller particle size has a wider surface, are more reactive, and more higher reactivity.

The results of the XRD analysis of INPs are shown in Exhibit 9.

Exhibit 9 shows that the solid nature of the synthesized INPs is amorphous. This is shown by the results of XRD analysis of INPs which did not show any diffraction peaks. A similar form was also reported

by Noruzi and Mousivand (2015) who used fan fir extract and Shahwan et al. (2011) who used green tea extract and rice bran extract. A similar form was also reported by Devatha et al. (2016) who used leaf extract and Fazlzadeh et al. (2017) who used plant extract.

The reaction between Fe^{2+} and polyphenols is shown in Exhibit 10.

Exhibit 10 shows the reaction between Fe^{2+} and polyphenols characterized by the presence of IR absorption by the OH group (phenol) in the 3471 cm^{-1} region. In this area, there is a shift of peaks from 3471 cm^{-1} to 3388 cm^{-1} . The shift from 3471 to 3388 cm^{-1} indicates the involvement of O-H functional groups. The peak shift from 1638 to 1628 cm^{-1} indicates that C = C aromatic compounds are involved in the nanoparticle synthesis process. The peak shift from 1466 to 1393 cm^{-1} indicates the involvement of the carboxyl group of RPE in the synthesis of INPs. The peak at 697 cm^{-1} corresponds to the C-H stretching of aromatic compounds.

Rambutan peel mainly contains pectin, cellulose, and hemicellulose as well as polyphenols. These polymers, especially polyphenols reduce Fe^{2+} to Fe° (Kokila et al., 2015). The reaction between RPE and copperas solution proceeds spontaneously to produce a black solid. RPE can reduce Fe^{2+} to Fe° as seen from the brown solution turning black. The results of the characterization of INPs show that the compound contains Fe° elements which are mostly spherical with a particle size of 10–70 nm. From these results, it can be concluded that the reaction between RPE and copperas solution produces INPs. The weight percentage of Fe synthesized by RPE is only 19.64%, but the use of rambutan peels can add value to unused waste that can cause environmental pollution.

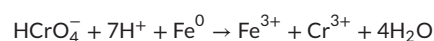
3.4 | Determination of efficiency and adsorption type of hexavalent chromium removal by INPs

a. The effect of pH

The effect of pH on hexavalent chromium removal was investigated from changes in pH of the solution of 3; 7 and 11 with different time intervals. The relationship between the initial pH of the solution and the percentage removal of hexavalent chromium is shown in Exhibit 11.

The percentage removal of hexavalent chromium can be seen in Exhibit 11, which increases as the pH decreases. The percentage removal of hexavalent chromium ions reached a maximum and remained relatively constant at 5 min at pH 3 and 20 min at pH 7 and 11. Among the various pH conditions, the maximum pH of removal was 3. At low pH (1–6), the dominant hexavalent chromium species is CrO_4^- and the surface of iron nanoparticles is positively charged. With increasing pH, there is a shift of HCrO_4^- species to CrO_4^{2-} species which are stable at $\text{pH} > 6$.

Hexavalent chromium removal by INPs involves the reduction of hexavalent chromium to trivalent chromium and the oxidation of Fe° to $\text{Fe}^{2+}/\text{Fe}^{3+}$. In this reaction, electron transfer from Cr^{6+} to Fe° occurs.



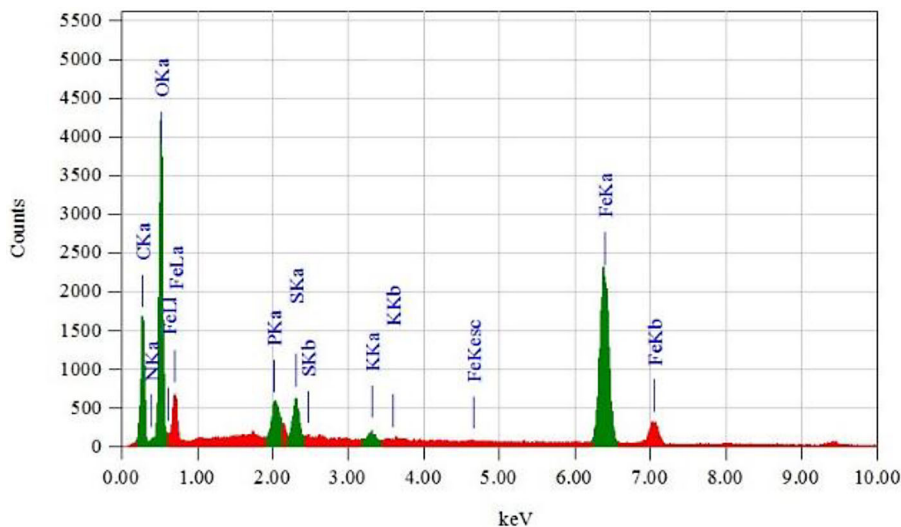


EXHIBIT 7 EDX spectrum of INPs. [Color figure can be viewed at wileyonlinelibrary.com]

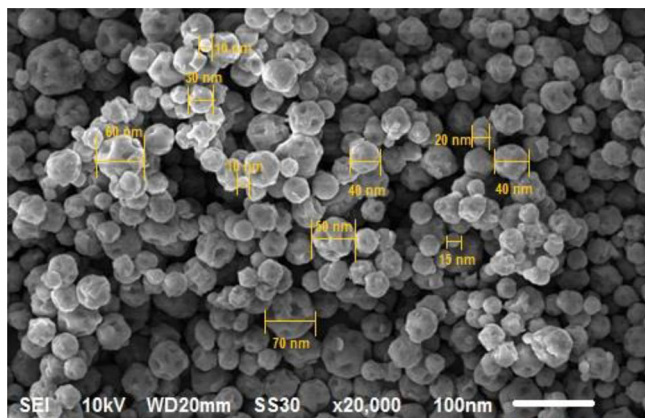


EXHIBIT 8 SEM analysis of INPs. [Color figure can be viewed at wileyonlinelibrary.com]

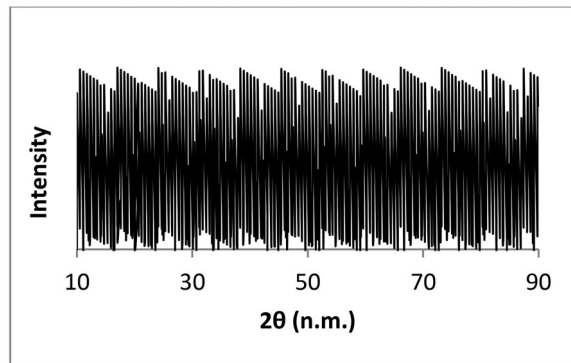
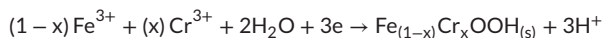


EXHIBIT 9 Results of XRD analysis of INPs.



Furthermore, Cr(III) precipitates as $\text{Cr}_x\text{Fe}_{1-x}(\text{OH})_3$ or $\text{Cr}_x\text{Fe}_{1-x}(\text{OOH})$, $x < 1$ (Poguberović et al., 2016). So the lower the pH the greater the adsorption of INPs on hexavalent chromium.

b. Effect of hexavalent chromium concentration

The relationship between the initial concentration of hexavalent chromium and hexavalent chromium removal efficiency is shown in Exhibit 12.

Exhibit 12 shows that the removal efficiency of hexavalent chromium decreased as the initial concentration of hexavalent chromium increased from 5 to 15 ppm. The decrease in hexavalent chromium removal percentage is due to INPs having limited activity, which will become saturated at a certain concentration (Wang et al., 2014). This result is similar to the results reported by Fazlzadeh et al.

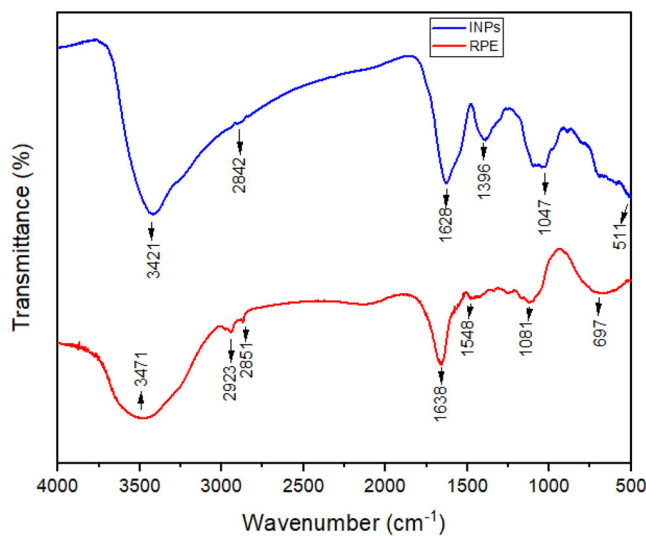


EXHIBIT 10 FTIR spectrum for INPs and RPE. [Color figure can be viewed at wileyonlinelibrary.com]

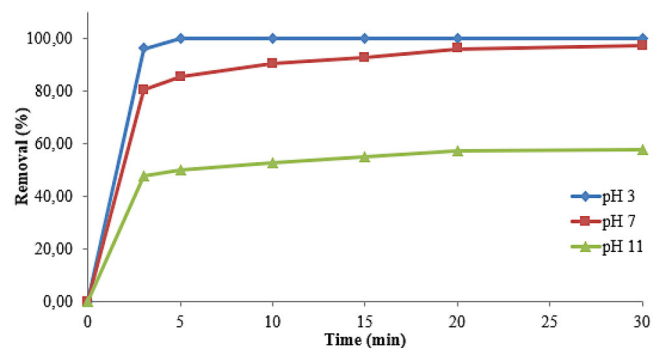


EXHIBIT 11 Effect of pH on hexavalent chromium removal with INPs. [Color figure can be viewed at [wileyonlinelibrary.com](#)]

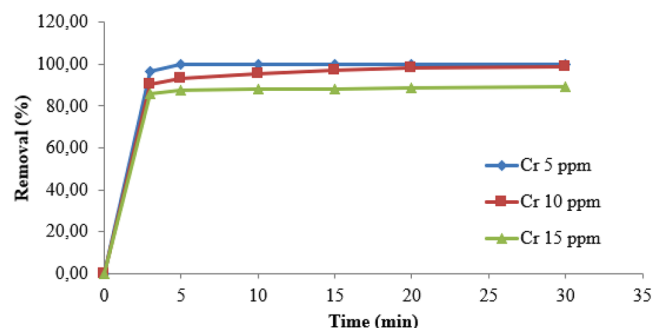


EXHIBIT 12 Effect of hexavalent chromium concentration on hexavalent chromium removal. [Color figure can be viewed at [wileyonlinelibrary.com](#)]

(2017) who used three plant extracts for hexavalent chromium removal and who used fertilizer production waste for hexavalent chromium removal. The percentage of hexavalent chromium removal decreased as the concentration of hexavalent chromium contaminant increased and showed high adsorption capacity of the synthesized INPs. The higher the hexavalent chromium concentration, the lower the percentage removal because INPs have a maximum limit in removing hexavalent chromium.

c. Effect of INP concentration

The results of the hexavalent chromium removal analysis with INPs varying the concentration of INPs are shown in Exhibit 13.

The hexavalent chromium removal percentage increased from 40.72% to 99.99% as the concentration of INPs increased from 0.01 to 0.15 g/100 mL. The hexavalent chromium removal percentage increases due to an increase in surface area location available for removal. Thus, the percentage removal of hexavalent chromium is higher in proportion to the greater concentration of iron nanoparticles.

d. Effect of contact time

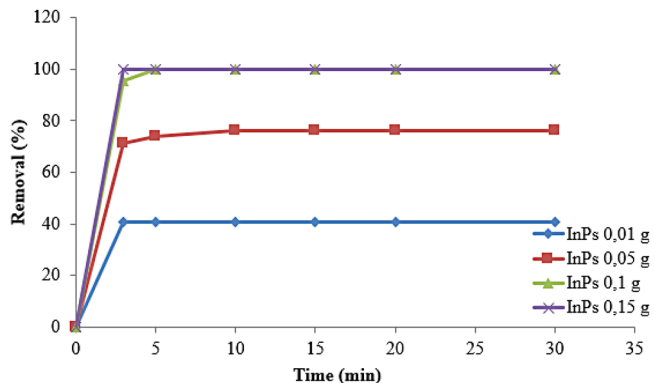


EXHIBIT 13 Effect of INPs concentration on hexavalent chromium removal with INPs. [Color figure can be viewed at [wileyonlinelibrary.com](#)]

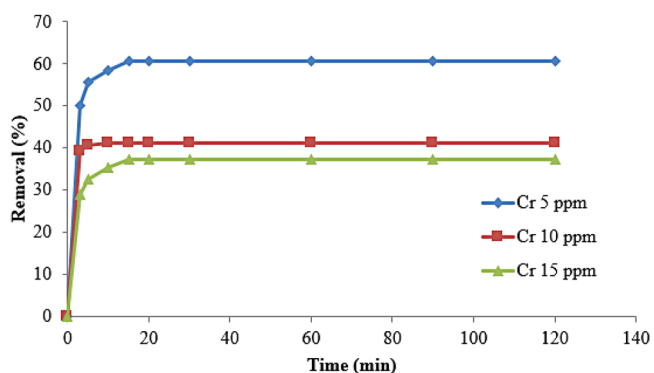


EXHIBIT 14 Effect of contact time on hexavalent chromium removal with INPs. [Color figure can be viewed at [wileyonlinelibrary.com](#)]

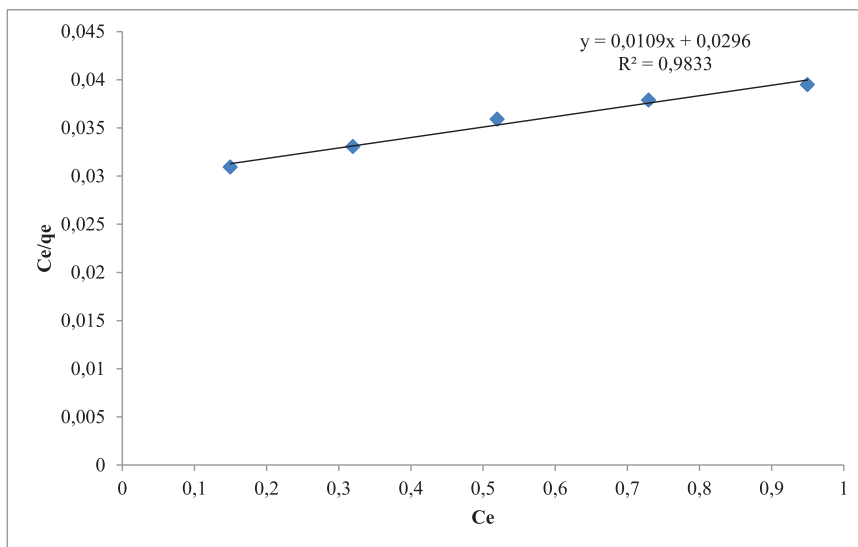
The results of the analysis of hexavalent chromium removal with INP contact time variation are shown in Exhibit 14.

The percentage removal of hexavalent chromium increased from 39.53% to 41.31% as the contact time increased from 3 to 120 min for an initial hexavalent chromium concentration of 10 mg/L. The percentage removal was optimal at 10 min. The longer the contact time between INPs and hexavalent chromium, the more hexavalent chromium is adsorbed until a certain time limit.

Based on the results from points a, b, c, and d above, the removal of hexavalent chromium (Cr(VI)) using iron nanoparticles is an effective and promising method to treat contaminated water. It is commonly found in industrial wastewater, and its removal is crucial to ensure safe drinking water and protect the environment (Cheng et al., 2023; Prema et al., 2022). INPs have gained attention as a potential remediation method due to their ability to reduce Cr(VI) to less toxic and less mobile trivalent chromium (Cr(III)) through a process called chemical reduction (Yang et al., 2023). Hexavalent chromium removal using INPs is generally effective, but it is necessary to consider certain factors, such as pH, temperature, and the presence of other contaminants, which can affect the efficiency of the process. Overall, the use of INPs for

EXHIBIT 15 Results of isotherm type determination of hexavalent chromium metal by INPs.

$C_{Cr(VI) \text{ Early}}$ (ppm)	C_e (ppm)	Q_e (mg/g)	C_e/q_e	$\text{Log } q_e$	$\text{Log } C_e$
5	0.15	4.85	0.031	0.686	-0.824
10	0.32	9.68	0.033	0.986	-0.495
15	0.52	14.48	0.036	1.161	-0.284
20	0.73	19.27	0.038	1.285	-0.137
25	0.95	24.05	1.381	1.381	-0.022

EXHIBIT 16 Langmuir adsorption isotherm curve of hexavalent chromium with INPs. [Color figure can be viewed at wileyonlinelibrary.com]

hexavalent chromium removal is a promising and effective technology (Garvasis et al., 2023; Rajapaksha et al., 2022).

e. Determination of adsorption isotherm type

Determination of adsorption isotherm type was done by entering equilibrium data into Equation (4) (Langmuir isotherm) and Equation (5) (Freundlich isotherm), the results of which are shown in Exhibit 15.

If a straight line is made using the Langmuir isotherm equation, the C_e/q_e versus C_e curve, and the Freundlich isotherm equation, the $\log C_e$ versus $\log q_e$ curve will be obtained as shown in Exhibits 16 and 17.

Exhibits 16 and 17 show that the adsorption equation of hexavalent chromium ions by INPs fulfills the Langmuir isotherm equation with $R^2 = 0.9833$ and the Freundlich isotherm equation with $R^2 = 0.9995$. This indicates that Langmuir and Freundlich's equations can be applied to the adsorption process of hexavalent chromium by INPs (Rahmani et al., 2011; Khatoon et al., 2013). The correlation coefficient (R^2) of Freundlich isotherm ($R^2 = 0.9995$) is more suitable than the Langmuir model ($R^2 = 0.9833$) for hexavalent chromium adsorption. This means that the Freundlich isotherm model is more suitable than the Langmuir isotherm model. This result is similar to the study of Poguberović et al. (2016) on the adsorption of As(III) and hexavalent chromium using INPs from oak, mulberry, and cherry leaf extracts which fit the Freundlich isotherm model. From the Langmuir isotherm straight line equation, $y = 0.0109x + 0.0296$, the adsorption capacity (q_{max}) of

INPs on hexavalent chromium can be determined from the intercept price $1/q_{max} = 0.0296$, so that the adsorption capacity price, q_{max} is 91.74 mg/g hexavalent chromium. Based on the price of R^2 , the adsorption process between INPs and hexavalent chromium takes place in a multilayer manner.

4 | CONCLUSION

The conclusions of this research are:

1. The level of copperas produced from iron scrap in the lathe workshop has a Fe content of $19.84 \pm 0.15\%$. These results meet SNI 06-4888-1998 standards regarding copperas quality requirements with a minimum Fe content of 19%.
2. Rambutan peel extract contains phenol compounds with a total phenol content of 877.39 ± 16.6 ppm/100 g mg/100 g rambutan peel. This result is equivalent to 441.42 mg GAE/100 g rambutan peel.
3. The characteristics of iron nanoparticles produced from the reaction of rambutan peel extract with copperas from iron scrap of the lathe workshop are on average spherical with a size of 10–70 nm.
4. Hexavalent chromium removal using INPs was maximum at pH 3.1, hexavalent chromium concentration of 5 ppm, INPs concentration of 0.10 g/100 mL, and contact time of 10 min. The adsorption

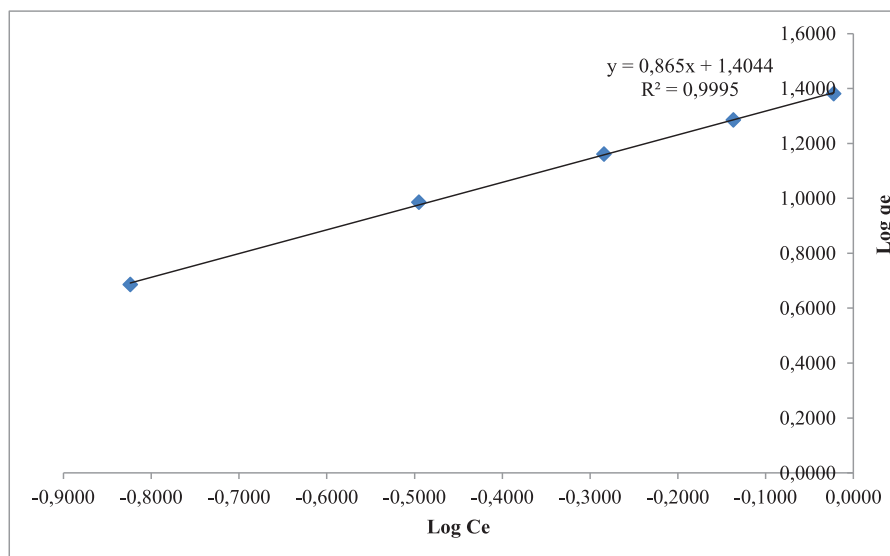


EXHIBIT 17 Freundlich isotherm curve of hexavalent chromium adsorption by INPs. [Color figure can be viewed at wileyonlinelibrary.com]

isotherm type of hexavalent chromium using INPs can take place chemically or physically. The correlation coefficient showed that the Freundlich model ($R^2 > 0.99$) was more suitable than the Langmuir model ($R^2 = 0.98$) with an adsorption capacity of 91.74 mg INPs/g hexavalent chromium. Overall, the use of INPs for hexavalent chromium removal is a promising and effective technology.

CONFLICT OF INTEREST STATEMENT

The authors declare that they have no competing interests.

DATA AVAILABILITY STATEMENT

The data that support the findings of this study are available in repository .setiabudi.ac.id at <http://repository.setiabudi.ac.id/cgi/users/home>. These data were derived from the following resources available in the public domain: [list resources and URLs].

ORCID

Sunardi Sunardi  <https://orcid.org/0000-0001-5060-736X>

REFERENCES

- Ahamed, I. N., Anbu, S., Vikraman, G., Nasreen, S., Muthukumari, M., & Kumar, M. M. (2016). Green synthesis of nano zerovalent iron particles (NZVI) for environmental remediation. *Life Science Archives*, 2(3), 549–554.
- Anouar, E. H., Gierschner, J., Duroux, J.-L., & Trouillas, P. (2015). UV /Visible spectra of natural polyphenols: A time-dependent density functional theory study. *Food Chemistry*, 131(1), 79–89. <https://doi.org/10.1016/j.foodchem.2011.08.034>
- Chang, D., Chen, T., Liu, H., Xi, Y., Qing, C., Xie, Q., & Frost, R. L. (2014). A new approach to prepare ZVI and its application in removal of Cr(VI) from aqueous solution. *Chemical Engineering Journal*, 244, 264–272. <https://doi.org/10.1016/j.cej.2014.01.095>
- Chen, T., Zhou, Z., Xu, S., Wang, H., & Lu, W. (2015). Adsorption behavior comparison of trivalent and hexavalent chromium on biochar derived from municipal sludge. *Bioresource Technology*, 190, 388–394.
- Cheng, X., Chen, J., Li, H., & Sheng, G. (2023). Preparation and evaluation of celite decorated iron nanoparticles for the sequestration performance of hexavalent chromium from aqueous solution. *Environmental Science and Pollution Research*, 30(23), 63535–63548. <https://doi.org/10.1007/S11356-023-26896-4/METRICS>
- Crane, R. A., & Scott, T. B. (2012). Nanoscale zero-valent iron: Future prospects for an emerging water treatment technology. *Journal of Hazardous Materials*, 211–212, 112–125. <https://doi.org/10.1016/j.jhazmat.2011.11.073>
- Devatha, C. P., Thalla, A. K., & Katte, S. Y. (2016). Green synthesis of iron nanoparticles using different leaf extracts for treatment of domestic waste water. *Journal of Cleaner Production*, 139, 1425–1435. <https://doi.org/10.1016/j.jclepro.2016.09.019>
- Etemadi, M., Samadi, S., Yazd, S. S., Jafari, P., Yousefi, N., & Aliabadi, M. (2017). Selective adsorption of Cr(VI) ions from aqueous solutions using Cr6+-imprinted Pebax/chitosan/GO/APTES nanofibrous adsorbent. *International Journal of Biological Macromolecules*, 95(December), 725–733. <https://doi.org/10.1016/j.ijbiomac.2016.11.117>
- Fazlzadeha, M., Rahmania, K., Zareib, A., Abdoallahzadeha, H., Nasiric, F., & Khosravi, R. (2017). A novel green synthesis of zero valent iron nanoparticles (NZVI) using three plant extracts and their efficient application for removal of Cr(VI) from aqueous solutions. *Advanced Powder Technology*, 28(1), 122–130.
- Fujioka, N., Suzuki, M., Kurosu, S., & Kawase, Y. (2016). Linkage of iron elution and dissolved oxygen consumption with removal of organic pollutants by nanoscale zero-valent iron: Effects of pH on iron dissolution and formation of iron oxide/hydroxide layer. *Chemosphere*, 144, 1738–1746. <https://doi.org/10.1016/j.chemosphere.2015.10.064>
- Garvasis, J., Prasad, A. R., Shamsheera, K. O., Nidheesh Roy, T. A., & Joseph, A. (2023). A facile one-pot synthesis of phyto-conjugate superparamagnetic magnetite nanoparticles for the rapid removal of hexavalent chromium from water bodies. *Materials Research Bulletin*, 160, 112130. <https://doi.org/10.1016/J.MATERRESBULL.2022.112130>
- Giri, S., Samanta, S., Maji, S., Ganguli, S., & Bhaumik, A. (2005). Magnetic properties of α -Fe₂O₃ nanoparticle synthesized by a new hydrothermal method. *Journal of Magnetism and Magnetic Materials*, 285(1–2), 296–302. <https://doi.org/10.1016/j.jmmm.2004.08.007>
- Harshiny, M., Iswarya, C. N., & Matheswaran, M. (2015). Biogenic synthesis of iron nanoparticles using *Amaranthus dubius* leaf extract as a

- reducing agent. *Powder Technology*, 286, 744–749. <https://doi.org/10.1016/j.powtec.2015.09.021>
- Isacfranklin, M., Dawoud, T., Ameen, F., Ravi, G., Yuvakkumar, R., Kumar, P., Hong, S. I., Velauthapillai, D., & Saravanakumar, B. (2020). Synthesis of highly active biocompatible ZrO₂ nanorods using a bioextract. *Ceramics International*, 46(16), 25915–25920. <https://doi.org/10.1016/j.ceramint.2020.07.076>
- Jiao, C., Cheng, Y., Fan, W., & Li, J. (2015). Synthesis of agar-stabilized nanoscale zero-valent iron particles and removal study of hexavalent chromium. *International Journal of Environmental Science and Technology*, 12(5), 1603–1612. <https://doi.org/10.1007/s13762-014-0524-0>
- Karnan, T., Arul, S., Selvakumar, S., Adinaveen, T., & Suresh, J. (2016). Visible light induced photocatalytic degradation of azo dye by Bi₂O₃ nanoparticles synthesized using greener route. *International Journal of Scientific & Engineering Research*, 7(8), 266–270.
- Karnan, T., & Selvakumar, S. A. S. (2016). Biosynthesis of ZnO nanoparticles using rambutan (*Nephelium lappaceum* L.) peel extract and their photocatalytic activity on methyl orange dye. *Journal of Molecular Structure*, 1125, 358–365. <https://doi.org/10.1016/J.MOLSTRUC.2016.07.029>
- Karnan, T., & Selvakumar, S. A. S. (2016). Biosynthesis of ZnO nanoparticles using rambutan (*Nephelium lappaceum* L.) peel extract and their photocatalytic activity on methyl orange dye. *Journal of Molecular Structure*, 1125, 358–365. <https://doi.org/10.1016/J.MOLSTRUC.2016.07.029>
- Kokila, T., Ramesh, P. S., & Geetha, D. (2015). Biosynthesis of silver nanoparticles from Cavendish banana peel extract and its antibacterial and free radical scavenging assay: A novel biological approach. *Applied Nanoscience*, 5(8), 911–920. <https://doi.org/10.1007/s13204-015-0401-2>
- Kumar, B., Smita, K., Angulo, Y., & Cumbal, L. (2016). Valorization of rambutan peel for the synthesis of silver-doped titanium dioxide (Ag/TiO₂) nanoparticles. *Green Processing and Synthesis*, 5(4), 371–377. <https://doi.org/10.1515/gps-2016-0003>
- Kumari, M., Pittman, C. U., & Mohan, D. (2015). Heavy metals [chromium (VI) and lead (II)] removal from water using mesoporous magnetite (Fe₃O₄) nanospheres. *Journal of Colloid and Interface Science*, 442, 120–132. <https://doi.org/10.1016/j.jcis.2014.09.012>
- Leili, M., Fazlzadeh, M., & Bhatnagar, A. (2018). Green synthesis of nano-zero-valent iron from Nettle and Thyme leaf extracts and their application for the removal of cephalixin antibiotic from aqueous solutions. *Environmental Technology (United Kingdom)*, 39(9), 1158–1172. <https://doi.org/10.1080/09593330.2017.1323956>
- Li, S., Wang, W., Liang, F., & Zhang, W. (2017). Heavy metal removal using nanoscale zero-valent iron (nZVI): Theory and application. *Journal of Hazardous Materials*, 322, 163–171. <https://doi.org/10.1016/j.jhazmat.2016.01.032>
- Machado, S., Pinto, S. L., Grosso, J. P., Nouws, H. P. A., Albergaria, J. T., & Delerue-Matos, C. (2013). Green production of zero-valent iron nanoparticles using tree leaf extracts. *The Science of the Total Environment*, 445–446, 1–8. <https://doi.org/10.1016/j.scitotenv.2012.12.033>
- Madhavi, V., Prasad, T., & Madhavi, G. (2013). Synthesis and spectral characterization of iron based micro and nanoparticles. *International Journal of Nanomaterials and Biostructures*, 3(2), 31–34. <https://doi.org/10.5829/idosi.ijee.2013.04.04.10>
- Mendez-Flores, A., Hernández-Almanza, A., Sáenz-Galindo, A., Morlett-Chávez, J., Aguilar, C., & Ascacio-Valdés, J. (2018). Ultrasound-assisted extraction of antioxidant polyphenolic compounds from *Nephelium lappaceum* L. (Mexican variety) husk. *Asian Pacific Journal of Tropical Medicine*, 11(12), 676. <https://doi.org/10.4103/1995-7645.248339>
- Mo, Y., Tang, Y., Wang, S., Lin, J., Zhang, H., & Luo, D. (2015). Green synthesis of silver nanoparticles using eucalyptus leaf extract. *Materials Letters*, 144(April 2015), 165–167. <https://doi.org/10.1016/j.matlet.2015.01.004>
- Mystrioti, C., Xanthopoulou, T. D., Tsakiridis, P., Papassiopi, N., & Xenidis, A. (2016). Comparative evaluation of five plant extracts and juices for nanoiron synthesis and application for hexavalent chromium reduction. *Science of The Total Environment*, 539, 105–113. <https://doi.org/10.1016/j.scitotenv.2015.08.091>
- Noruzi, M., & Mousivand, M. (2015). Instantaneous Green Synthesis of Zerovalent Iron Nanoparticles by Thuja orientalis Extract and Investigation of Their Antibacterial Properties. *Journal of Applied Chemistry Research*, 9(2), 37–50.
- O'Carroll, D., Sleep, B., Krol, M., Boparai, H., & Kocur, C. (2013). Nanoscale zero valent iron and bimetallic particles for contaminated site remediation. *Advances in Water Resources*, 51, 104–122.
- Petcharoen, K., & Sirivat, A. (2012). Synthesis and characterization of magnetite nanoparticles via the chemical co-precipitation method. *Materials Science and Engineering B: Solid-State Materials for Advanced Technology*, 177(5), 421–427. <https://doi.org/10.1016/j.mseb.2012.01.003>
- Poguberović, S. S., Krčmar, D. M., Maletić, S. P., Kónya, Z., Pilipović, D. D. T., Kerkez, D. V., & Rončević, S. D. (2016). Removal of As(III) and Cr(VI) from aqueous solutions using “green” zero-valent iron nanoparticles produced by oak, mulberry and cherry leaf extracts. *Ecological Engineering*, 90, 42–49. <https://doi.org/10.1016/j.ecoleng.2016.01.083>
- Prasad, K. S., Gandhi, P., & Selvaraj, K. (2014). Synthesis of green nano iron particles (GnIP) and their application in adsorptive removal of As(III) and As(V) from aqueous solution. *Applied Surface Science*, 317, 1052–1059. <https://doi.org/10.1016/j.apsusc.2014.09.042>
- Prema, P., Nguyen, V. H., Venkatachalam, K., Murugan, J. M., Ali, H. M., Salem, M. Z. M., Ravindran, B., & Balaji, P. (2022). Hexavalent chromium removal from aqueous solutions using biogenic iron nanoparticles: Kinetics and equilibrium study. *Environmental Research*, 205, 112477. <https://doi.org/10.1016/J.ENVRES.2021.112477>
- Rajapaksha, A. U., Selvasembian, R., Ashiq, A., Gunarathne, V., Ekanayake, A., Perera, V. O., Wijesekera, H., Mia, S., Ahmad, M., Vithanage, M., & Ok, Y. S. (2022). A systematic review on adsorptive removal of hexavalent chromium from aqueous solutions: Recent advances. *Science of the Total Environment*, 809, 152055. <https://doi.org/10.1016/J.SCITOTENV.2021.152055>
- Ravikumar, K. V. G., Kumar, D., Rajeshwari, A., Madhu, G. M., Mrudula, P., Chandrasekaran, N., & Mukherjee, A. (2016). A comparative study with biologically and chemically synthesized nZVI: Applications in Cr (VI) removal and ecotoxicity assessment using indigenous microorganisms from chromium-contaminated site. *Environmental Science and Pollution Research*, 23(3), 2613–2627. <https://doi.org/10.1007/s11356-015-5382-x>
- Saif, S., Tahir, A., & Chen, Y. (2016). Green synthesis of iron nanoparticles and their environmental applications and implications. *Nanomaterials (Basel, Switzerland)*, 6(11), 209. <https://doi.org/10.3390/nano6110209>
- Shahwan, T., Abu Sirriah, S., Nairat, M., Boyacı, E., Eroğlu, A. E., Scott, T. B., & Hallam, K. R. (2011). Green synthesis of iron nanoparticles and their application as a Fenton-like catalyst for the degradation of aqueous cationic and anionic dyes. *Chemical Engineering Journal*, 172(1), 258–266. <https://doi.org/10.1016/j.cej.2011.05.103>
- Sheng, G., Hu, J., Li, H., Li, J., & Huang, Y. (2016). Enhanced sequestration of Cr(VI) by nanoscale zero-valent iron supported on layered double hydroxide by batch and XAFS study. *Chemosphere*, 148, 227–232. <https://doi.org/10.1016/j.chemosphere.2016.01.035>
- Solimanzadeh, A., Fekri, M., Bakhtyari, S., & Mehrizi, M. H. (2016). Biosynthesis of iron nanoparticles and their application in removing phosphorus from aqueous solutions. *Chemistry and Ecology*, 32(3), 286–300.
- Thitilertdecha, N., & Rakariyatham, N. (2011). Phenolic content and free radical scavenging activities in rambutan during fruit maturation. *Scientia Horticulturae*, 129(2), 247–252. <https://doi.org/10.1016/J.SCIENTA.2011.03.041>
- Thitilertdecha, N., Teerawutgulrag, A., Kilburn, J. D., Rakariyatham, N., Thitilertdecha, N., Teerawutgulrag, A., Kilburn, J. D., & Rakariyatham, N. (2010). Identification of major phenolic compounds from *Nephelium lappaceum* L. and their antioxidant activities. *Molecules (Basel, Switzerland)*, 15(3), 1453–1465. <https://doi.org/10.3390/molecules15031453>

- Thitilertdecha, N., Teerawutgulrag, A., & Rakariyatham, N. (2008). Antioxidant and antibacterial activities of *Nephelium lappaceum* L. extracts. *LWT—Food Science and Technology*, 41(10), 2029–2035. <https://doi.org/10.1016/J.LWT.2008.01.017>
- Tsang, S. C., Yu, C. H., Gao, X., & Tam, K. (2006). Silica-encapsulated nanomagnetic particle as a new recoverable biocatalyst carrier. *Journal of Physical Chemistry B*, 110(34), 16914–16922. <https://doi.org/10.1021/jp062275s>
- Wang, X., Wang, A., Ma, J., & Fu, M. (2017). Facile green synthesis of functional nanoscale zero-valent iron and studies of its activity toward ultrasound-enhanced decolorization of cationic dyes. *Chemosphere*, 166, 80–88. <https://doi.org/10.1016/j.chemosphere.2016.09.056>
- Wang, Z., Fang, C., & Megharaj, M. (2014). Characterization of iron – polyphenol nanoparticles synthesized by three plant extracts and their fenton oxidation of azo dye. *ACS Sustainable Chemistry & Engineering*, 2(4), 1–4. <https://doi.org/10.1021/sc500021n>
- Wei, Y., Fang, Z., Zheng, L., Tan, L., & Tsang, E. P. (2016). Green synthesis of Fe nanoparticles using *Citrus maxima* peels aqueous extracts. *Materials Letters*, 185, 384–386. <https://doi.org/10.1016/j.matlet.2016.09.029>
- Xu, J., Gao, N., Zhao, D., Yin, D., Zhang, H., Gao, Y., & Shi, W. (2015). Comparative study of nano-iron hydroxide impregnated granular activated carbon (Fe–GAC) for bromate or perchlorate removal. *Separation and Purification Technology*, 147, 9–16. <https://doi.org/10.1016/j.seppur.2015.03.052>
- Yang, H., Kim, N., & Park, D. (2023). Ecotoxicity study of reduced-Cr(III) generated by Cr(VI) biosorption. *Chemosphere*, 332, 138825. <https://doi.org/10.1016/J.CHEMOSPHERE.2023.138825>
- Yoon, S.-Y., Lee, C.-G., Park, J.-A., Kim, J.-H., Kim, S.-B., Lee, S.-H., & Choi, J.-W. (2014). Kinetic, equilibrium and thermodynamic studies for phosphate adsorption to magnetic iron oxide nanoparticles. *Chemical Engineering Journal*, 236, 341–347. <https://doi.org/10.1016/j.cej.2013.09.053>
- Yuan, N., Zhang, G., Guo, S., & Wan, Z. (2016). Enhanced ultrasound-assisted degradation of methyl orange and metronidazole by rectorite-supported nanoscale zero-valent iron. *Ultrasonics Sonochemistry*, 28, 62–68. <https://doi.org/10.1016/j.ultsonch.2015.06.029>
- Yuvakkumar, R., Suresh, J., Saravanakumar, B., Joseph Nathanael, A., Hong, S. I., & Rajendran, V. (2015). Rambutan peels promoted biomimetic synthesis of bioinspired zinc oxide nanochains for biomedical applications. *Spectrochimica Acta—Part A: Molecular and Biomolecular Spectroscopy*, 137, 250–258. <https://doi.org/10.1016/j.saa.2014.08.022>
- Zhuang, Y., Ma, Q., Guo, Y., & Sun, L. (2017). Protective effects of rambutan (*Nephelium lappaceum*) peel phenolics on H₂O₂-induced oxidative damages in HepG2 cells and D-galactose-induced aging mice. *Food and Chemical Toxicology*, 108, 554–562. <https://doi.org/10.1016/j.fct.2017.01.022>

How to cite this article: Sunardi, S., Sumardiyono, S., Mardiyono, M., Hidayati, N., & Soebiyanto, S. (2024). Utilization of Iron Scrap into Copperas and Rambutan (*Nephelium lappaceum* L.) Peel Extract into Environmentally Friendly Iron Nanoparticles for Hexavalent Chromium Removal and its Kinetics. *Environmental Quality Management*, 33(3), 531–542. <https://doi.org/10.1002/tqem.22153>